ELSEVIER

Journal of Nuclear Materials 219 (1995) 143–151

journal of nuclear materials

Why is magnesia spinel a radiation-resistant material?

C. Kinoshita [a], K. Fukumoto [b], K. Fukuda [a], F.A. Garner [c], G.W. Hollenberg [c]

[a] *Department of Nuclear Engineering, Kyushu University 36, Fukuoka 812, Japan*
[b] *Institute for Materials Research, Tohoku University, Sendai 980, Japan*
[c] *Materials Sciences Department, Pacific Northwest Laboratory, Richland, WA 99352, USA*

Abstract

Side-by-side irradiation of stoichiometric $MgAl_2O_4$ and α-Al_2O_3 in JOYO shows that the radiation-induced microstructural evolution to exposure of ≤ 6 dpa proceeds by very different paths in these two materials. The large difference in dislocation loop evolution appears to account for the ease of void swelling in α-Al_2O_3 and the strong resistance to void formation in $MgAl_2O_4$. Irradiation of $MgAl_2O_4$ to much higher exposure (22–230 dpa) in FFTF confirms the details of the dislocation evolution, which involves a progressive change in Burgers vector and habit plane as interstitial loops increase in size. Constraints unique to the $MgAl_2O_4$ crystal structure do not allow the formation of dislocation network structures that favor swelling.

1. Introduction

It has recently become evident that $MgAl_2O_4$ spinel, which has been proposed to serve as insulators and RF windows in fusion reactors, exhibits a strong resistance to void swelling during neutron irradiation. This resistance is in contrast to the response of α-Al_2O_3, which swells catastrophically at relatively low neutron exposures [1]. The superior resistance of $MgAl_2O_4$ has been attributed to a variety of factors. First, it has been noted that loops formed in this material are resistant to unfaulting and therefore do not form dislocation networks which promote high rates of void growth [2]. Thus, direct recombination of vacancies and interstitials is thought to be the dominant mode of defect accommodation, especially in nonstoichiometric $MgO \cdot nAl_2O_3$ ($n > 1.00$). It also appears that swelling does not develop in part due to an inherent suppression of loop formation arising from the large critical size of loop nuclei in $MgAl_2O_4$ [3]. The ratio of ionizing to displacive radiation may also play a role in the nucleation and growth of defect clusters. Zinkle noted that no clusters were found in ion-irradiated spinel for ionizing to displacive ratios larger than 10 [4]. At this time, however, the dominant factor or factors leading to loop suppression and swelling resistance in $MgAl_2O_4$ has not yet been determined.

In order to provide additional insight on the origin of the swelling resistance, two experiments were conducted. The first involved a side-by-side irradiation of both $MgAl_2O_4$ and α-Al_2O_3 to relatively low neutron exposure, followed by microscopy examination to explore the differences in microstructural evolution. The second experiment involved a comparable examination of $MgAl_2O_4$ specimens irradiated to much higher exposures in another reactor, in order to see whether trends observed at lower fluences in $MgAl_2O_4$ persisted at higher exposure levels.

2. Experimental procedure

In both irradiation experiments, the single crystals employed were very nearly stoichiometric. In the first irradiation experiment conducted in the JOYO fast breeder test reactor, the Linde Czochralski-grown $MgAl_2O_4$ specimen were supplied by F.W. Clinard, Jr. and were used in his earlier studies. The details of impurity levels and preparation have been presented earlier [1–3]. The α-Al_2O_3 single crystals were also Cz-grown and were supplied by Kyocera Co. Each of these crystals was cut into disks 3 mm in diameter using a diamond cutter and then mechanically thinned to 0.2 mm thickness.

SSDI 0022-3115(94)00388-2

Table 1
Specimens and irradiation conditions in JOYO and FFTF. Total dpa is estimated based on measured neutron fluences and assuming an equivalence of 1 dpa per 10^{25} n/m^2, $E > 0.1$ MeV [5]

Specimens	$MgO \cdot Al_2O_3$ (Linde) α-Al_2O_3 (Kyocera)	$MgO \cdot Al_2O_3$ (Union Carbide)
Reactor	JOYO	FFTF
Irradiation temperatures (K)	673, 773, 873	658, 1023
Neutron fluences (nm^{-2}, $E > 0.1$ MeV)	$(0.76–64)\times10^{24}$	$(220–2300)\times10^{24}$
Calculated dpa	0.08–6.3	22–230

In the second experiment, single crystal specimens of highly stoichiometric $MgAl_2O_4$ produced by Union Carbide were prepared in the form of 10 mm disks of 0.5 mm thickness by R.C. Bradt. They were subsequently irradiated to very high exposures with active temperature control to ± 5 K in the Materials Open Test Assembly (MOTA) of the Fast Flux Test Facility (FFTF). The details of specimen preparation and irradiation have been published elsewhere [5,6]. A brief summary of irradiation conditions is presented in Table 1.

After irradiation, the specimens were either crushed into powder using an alumina mortar and pestle or ground into powder using diamond paper. The powder was then suspended in n-propyl alcohol and the suspension was placed on microscopy microgrids using a syringe. The grids were dried in vacuum and then placed in a JEM-2000EX microscope operated at 200 kV. Powder specimens produced from unirradiated specimens were also examined to confirm that the observed microstructures did not arise in part from the pulverization process.

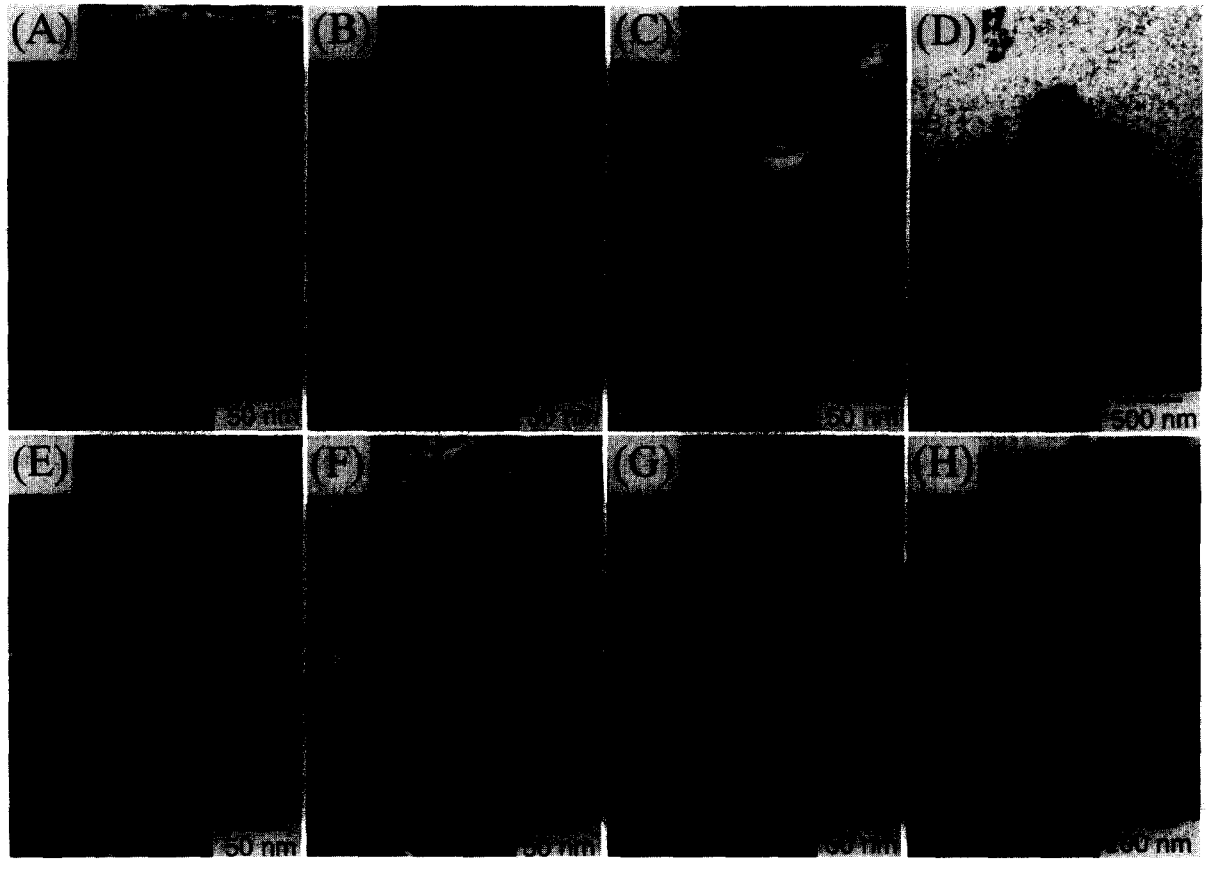

Fig. 1. Typical examples of electron micrographs showing interstitial dislocation loops in $MgAl_2O_4$ irradiated in JOYO to (a) 7.6×10^{23} n/m^2 at 673 K, (b) 7.5×10^{24} n/m^2 at 673 K, (c) 7.5×10^{24} n/m^2 at 773 K, (d) 7.5×10^{24} n/m^2 at 873 K, (e) 5.49×10^{25} n/m^2 at 673 K, (f) 5.49×10^{25} n/m^2 at 773 K, (g) 6.3×10^{25} n/m^2 at 673 K and (h) 6.2×10^{25} n/m^2 at 773 K.

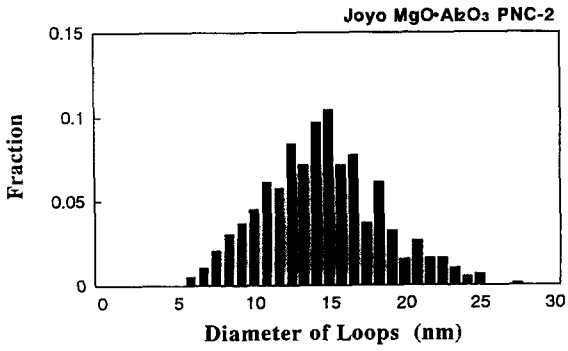

Fig. 2. The size distribution of loops observed in $MgAl_2O_4$ irradiated at 673 K to 7.5×10^{24} n/m^2 in JOYO.

3. Experimental results

3.1. $MgAl_2O_4$ irradiated in JOYO

Fig. 1 shows typical microstructures of defect clusters in $MgAl_2O_4$ irradiated in JOYO. At the lowest temperature, 673 K, and the lowest neutron fluence, 7.6×10^{23} n/m^2, no visible defect clusters were observed, but defect clusters were observed in the form of dislocation loops at higher temperatures and higher fluence levels. All fluences described in this paper are for neutrons with $E > 0.1$ MeV. Figs. 2 and 3 show examples of the size distribution of loops for irradiation at 773 K to fluences of 7.5×10^{24} and 5.49×10^{25} n/m^2, showing a Gaussian distribution and a bimodal distribution, respectively. The bimodal size distribution of loops for higher fluence irradiation, which required several sequences of start-up and shut-down operations of the reactor, is considered to arise from temperature transients during irradiation. The larger loops are thought to represent the intrinsic nucleation and growth process of loops in $MgAl_2O_4$ during isothermal irradiation. The smaller loops are thought to have nucleated at lower temperatures during shut-downs of the reactor. It is of great importance to pay attention to the disturbing effect of small details of temperature history

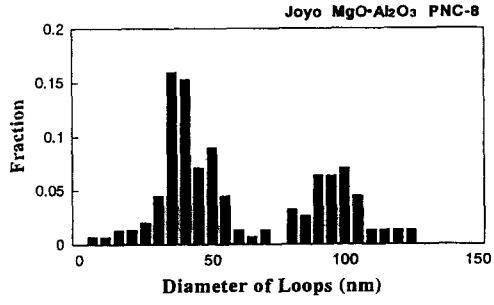

Fig. 3. The size distribution of loops in $MgAl_2O_4$ irradiated in JOYO at 773 K to 5.49×10^{25} n/m^2.

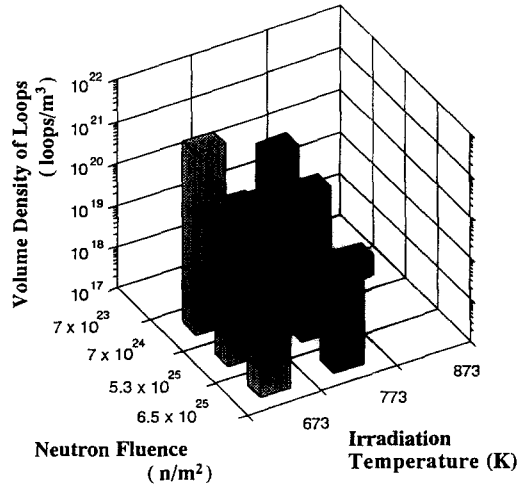

Fig. 4. The volume density of dislocation loops formed in $MgAl_2O_4$ irradiated with neutrons in JOYO as functions of irradiation temperature and neutron fluence.

for understanding the kinetic behavior of point defects during irradiation, as pointed out for irradiation of metals by Kiritani et al. [7] and Garner et al. [8].

The density and the mean diameter of dislocation loops were measured and they are shown as functions of irradiation temperature and neutron fluence in Figs. 4 and 5, respectively. The mean diameter of dislocation loops increases with increasing irradiation temperature and neutron fluence, being larger than 200 nm for irradiation to 6.15×10^{25} n/m^2 at 773 K. The microstructure of the defect clusters changes drastically at 873 K compared to those at 673 and 773 K, forming clusters of partially faulted dislocation loops on all six {110} planes. This type of defect was originally found

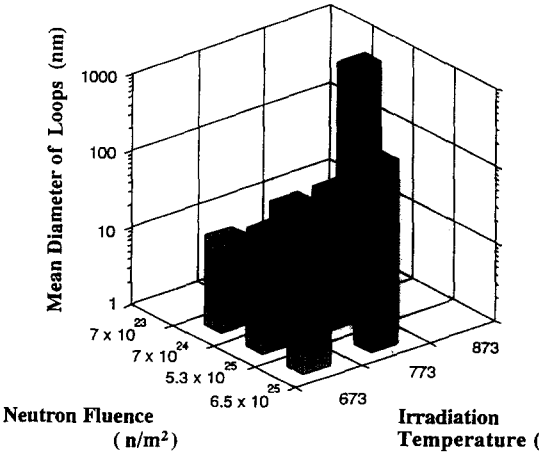

Fig. 5. The mean diameter of dislocation loops formed in $MgAl_2O_4$ irradiated with neutrons in JOYO as functions of irradiation temperature and neutron fluence.

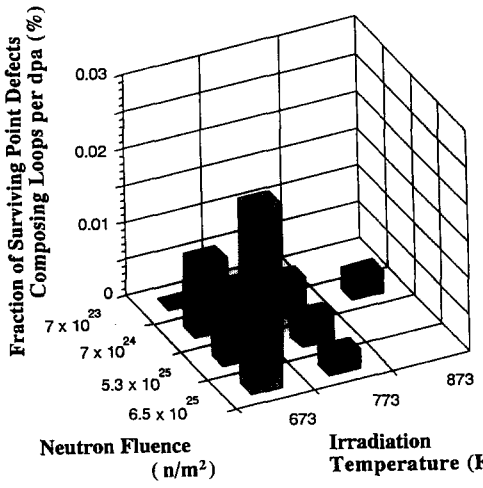

Fig. 6. The corresponding fraction of displaced atoms retained in the form of dislocation loops in neutron irradiated $MgAl_2O_4$ in JOYO as functions of irradiation temperature and neutron fluence.

by Clinard et al. and named as 'rosettes' [3]. No rosettes have been observed at 673 and 773 K. The fractions of displacements retained in the form of dislocation loops were calculated from the results in Figs. 4 and 5 and are shown as functions of irradiation temperature and neutron fluence in Fig. 6. As the irradiation temperature increases, the fraction tends to decrease, ranging from 0.02% down to 0.002% under the irradiation conditions described in Figs. 4 and 5. It is clear that the loop formation in neutron irradiated $MgAl_2O_4$ is strongly suppressed, compared with that in metals or in α-Al_2O_3 [1,9].

In order to obtain an insight into the mechanism of the nucleation and growth of dislocation loops, the Burgers vector ($\boldsymbol{b}$), the habit plane and the nature of the dislocation loops were determined, based on the $\boldsymbol{g}\cdot\boldsymbol{b}$ analysis, the inside–outside contrast method and the trace analysis [10–12]. Three different types of interstitial loops were found, with Burgers vectors, $\frac{1}{6}\langle 111\rangle$, $\frac{1}{4}\langle 110\rangle$ and $\frac{1}{2}\langle 110\rangle$. The Burgers vectors of the loops were found to depend on the size of the loops. With increasing neutron fluence, loops grew and changed their Burgers vectors and habit planes. To exclude the disturbing effect of temperature history during irradiation on the nucleation and growth process of loops, the diameter of loops, irrespective of the irradiation temperature, was found to be a good correlation parameter. Fig. 7 shows the fraction of each type of Burgers vector as a function of the diameter of the loops. The Burgers vector of each loop clearly changes from $\frac{1}{6}\langle 111\rangle$ to $\frac{1}{4}\langle 110\rangle$ and then to $\frac{1}{2}\langle 110\rangle$ as it grows. The critical diameter for the former and the latter transformation is 10–30 nm and is extrapolated to be

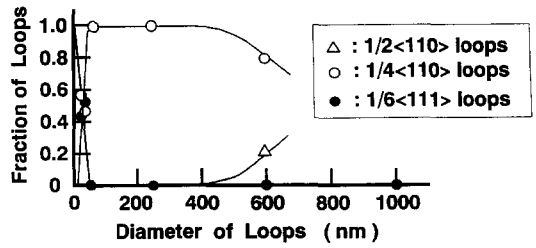

Fig. 7. The fractional variation of loops having Burgers vectors $\frac{1}{6}\langle 111\rangle$, $\frac{1}{4}\langle 110\rangle$ and $\frac{1}{2}\langle 110\rangle$ in $MgAl_2O_4$ after irradiation with neutrons in JOYO as a function of their diameter.

about 800 nm, respectively. The habit plane of $\frac{1}{4}[110]$ loops also changes with increasing diameter of loops, as shown in Fig. 8. The smallest loops with diameter of about 20 nm are on (111) planes, intermediate loops of about 200 to 600 nm are on the (101) and (110) planes, loops larger than 600 to 800 nm are dominantly $\frac{1}{4}[110](110)$ prismatic loops, and loops larger than about 800 nm are $\frac{1}{2}[110](110)$ perfect loops.

3.2. $MgAl_2O_4$ irradiated in FFTF

Typical examples of weak-beam dark-field images from $MgAl_2O_4$ specimens irradiated at 658 and 1023 K to 2.2×10^{26} and 2.17×10^{27} n/m^2, respectively, are shown in Fig. 9. The general dislocation structure for irradiation at 658 K consists of $\frac{1}{4}[110]$ type interstitial loops on the (111) and (110) planes and is essentially analogous to that obtained after irradiation in JOYO. Irradiation at 1023 K up to higher fluences, on the other hand, induces stacking fault networks formed by stacking faults on six equivalent {110} planes. The displacement vector of the stacking faults was determined by contrast analysis to be $\frac{1}{4}\langle 110\rangle$ on {110} planes. Although these stacking fault networks are similar to the ones found by Hobbs and Clinard [3], we have not observed $\frac{1}{2}[110](110)$ perfect loops also found by Hobbs and Clinard [3]. The loop evolution depends not only on size of loops but also on reactor for irradiation. Transmutation elements possibly affect the stacking

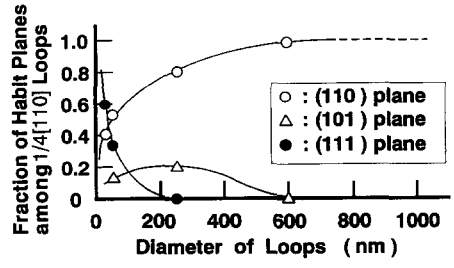

Fig. 8. The fractional variation of $\frac{1}{4}\langle 110\rangle$ loops lying on the (111), (101) and (110) planes in $MgAl_2O_4$ after irradiation with neutrons in JOYO, as a function of their diameter.

fault energy, though more experiments are required for getting the concluding remark on the loop evolution in different reactors.

No voids were observed in the specimens irradiated at 1023 K to 5.6×10^{26} n/m^2, but tiny voids 2–3 nm in diameter were found along the $\frac{1}{4}\langle 110\rangle\{110\}$ stacking faults at 1.38×10^{27} n/m^2, as shown in Fig. 10. The voids were confirmed to exhibit phase contrast variations upon changing from underfocus to overfocus using kinematical diffraction conditions. Fig. 10 also shows 6–8 nm voids in the matrix of the crystal irradiated to 2.17×10^{27} n/m^2. The density of voids was estimated to be 4×10^{24} voids/m^3, leading to void swelling of only 0.07%. This value agrees with macroscopic swelling measurements [5,6]. More comprehensive measurements are presented elsewhere [13].

3.3. α-Al_2O_3 irradiated in JOYO

As for the neutron irradiation behavior of α-Al_2O_3, other studies [1,14–17] have shown that irradiation results in the formation of interstitial dislocation loops with a Burgers vector of $\boldsymbol{b} = \frac{1}{3}\langle 10\bar{1}1\rangle$ that lie on both the $\{10\bar{1}0\}$ and (0001) planes. Along with formation of dislocation loops and networks, the studies of Clinard et al. [1] and Wilks et al. [14,15] and the more recent studies of Youngman et al. [17] have found the presence of voids. A similar behavior was observed in this study. Fig. 11 shows defect clusters formed in α-Al_2O_3 irradiated at 673, 773 and 873 K in JOYO. The interstitial clusters grow into well defined interstitial dislocation loops and form dislocation networks with increasing irradiation temperature and fluence. Fig. 12 further shows the microstructure of α-Al_2O_3 irradiated at 673 K to 5.49×10^{25} n/m^2, which consists of a high density of network dislocations coexisting with a high density of small voids. In this figure, the dislocation network is imaged using weak-beam dark-field conditions and the voids are imaged using kinematical bright-field conditions.

Three types of interstitial loops, $\frac{1}{3}[0001](0001)$, $\frac{1}{3}\langle 10\bar{1}0\rangle\{10\bar{1}0\}$ and $\frac{1}{3}\langle 10\bar{1}1\rangle(0001)$, were formed in α-Al_2O_3 as expected from earlier studies. The size distribution of each type of loop is plotted in Fig. 13 for three different neutron fluences at 673 K. The size of loops increases with increasing fluence, changing the relative population of each type of loop. Upon growing, the population of $\frac{1}{3}\langle 10\bar{1}1\rangle(0001)$ type of loops increases, with a corresponding decrease in the $\frac{1}{3}[0001](0001)$ and $\frac{1}{3}\langle 10\bar{1}0\rangle\{10\bar{1}0\}$ types of loops. This confirms the reactions proposed by Youngman et al. [15]; in which $\frac{1}{3}[0001]$ and $\frac{1}{3}\langle 10\bar{1}0\rangle$ loops unfault by shearing in the loop plane via the following reactions:

$$\underset{\text{(faulted loop)}}{\tfrac{1}{3}[0001](0001)} + \underset{\text{(partial shear)}}{\tfrac{1}{3}\langle 10\bar{1}0\rangle} \rightarrow \underset{\text{(unfaulted loop)}}{\tfrac{1}{3}\langle 10\bar{1}1\rangle(0001)},$$

$$\tfrac{1}{3}\langle 10\bar{1}0\rangle\{10\bar{1}0\} + \tfrac{1}{3}[0001] \rightarrow \tfrac{1}{3}\langle 10\bar{1}1\rangle\{10\bar{1}0\}.$$

4. Discussion

From the irradiation experiments conducted in both JOYO and FFTF, it appears that the nucleation and growth of loops in neutron irradiated $MgAl_2O_4$ follows the following steps;

$$\tfrac{1}{6}[111](111) \rightarrow \tfrac{1}{4}[110](111) \rightarrow \tfrac{1}{4}[110](101) \rightarrow \tfrac{1}{4}[110](110) \rightarrow \tfrac{1}{2}[110](110),$$

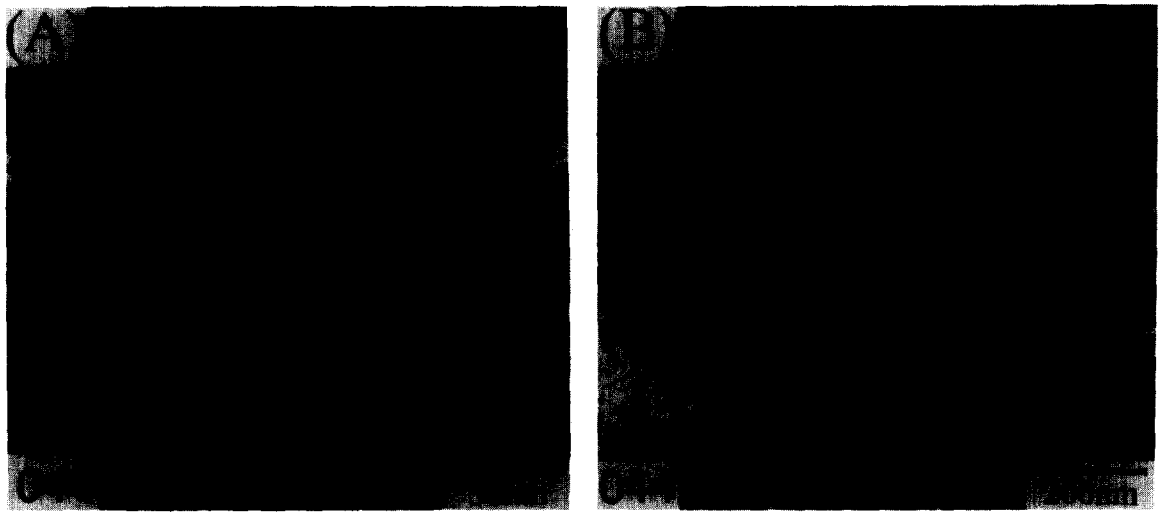

Fig. 9. Typical examples of weak-beam dark-field micrographs showing (A) $\frac{1}{4}[110](111)$ and $\frac{1}{4}[110](110)$ types of interstitial dislocation loops, and (B) stacking fault networks bounded by stacking faults on six equivalent {110} planes in $MgAl_2O_4$ irradiated in FFTF to (a) 2.2×10^{26} n/m^2 at 658 K and (b) 2.17×10^{27} n/m^2 at 1023 K, respectively.

changing their character as they grow larger. At lower neutron fluence levels and lower temperatures, unstable nuclei of $\frac{1}{6}[111]$ loops appear and a few of them grow into well defined loops. The elimination of $\frac{1}{6}\langle 111\rangle$ loops has been observed in other studies. For instance, such loops were induced by 6 keV Ar^+ ions and were eliminated during illumination with 100 to 1000 keV electrons [18]. It has been considered that the $\frac{1}{6}\langle 111\rangle$ loop has the anion and cation faults and cannot preserve stoichiometry and charge balance in either normal or inverse spinel [1,3]. Because of the nonstoichiometric component involved in the construction of $\frac{1}{6}\langle 111\rangle$ loops, they are unstable. However, partial inversion of inserted cation layers makes $\frac{1}{6}\langle 111\rangle$ loops stable against any deviation from either stoichiometry or charge neutrality.

The nucleation of $\frac{1}{6}\langle 111\rangle$ loops may be easier than that of $\frac{1}{4}\langle 110\rangle$ loops, because the $\frac{1}{6}\langle 111\rangle$ loop has a smaller Burgers vector than does the $\frac{1}{4}\langle 110\rangle$ loop, and the nucleus of $\frac{1}{6}\langle 111\rangle$ loops allows varying compositions [3,19]. On the other hand, it is possible that the stacking sequence of (111) or (101) planes preserves their stoichiometry by partly changing cation distributions, a process referred to as 'cation disordering'. The stacking sequence of $\frac{1}{6}[111](111)$ has both anion and cation faults and those of $\frac{1}{4}[110](111)$ and $\frac{1}{4}[110](101)$ have only cation faults in spinel crystals [19,20]. The changes in Burgers vectors and habit planes of loops during growth is strongly controlled by the stacking fault energy. The transition from $\frac{1}{6}[111](111)$ to $\frac{1}{4}[110](111)$ proceeds in order to reduce the deviation from electrical neutrality arising from the composi-

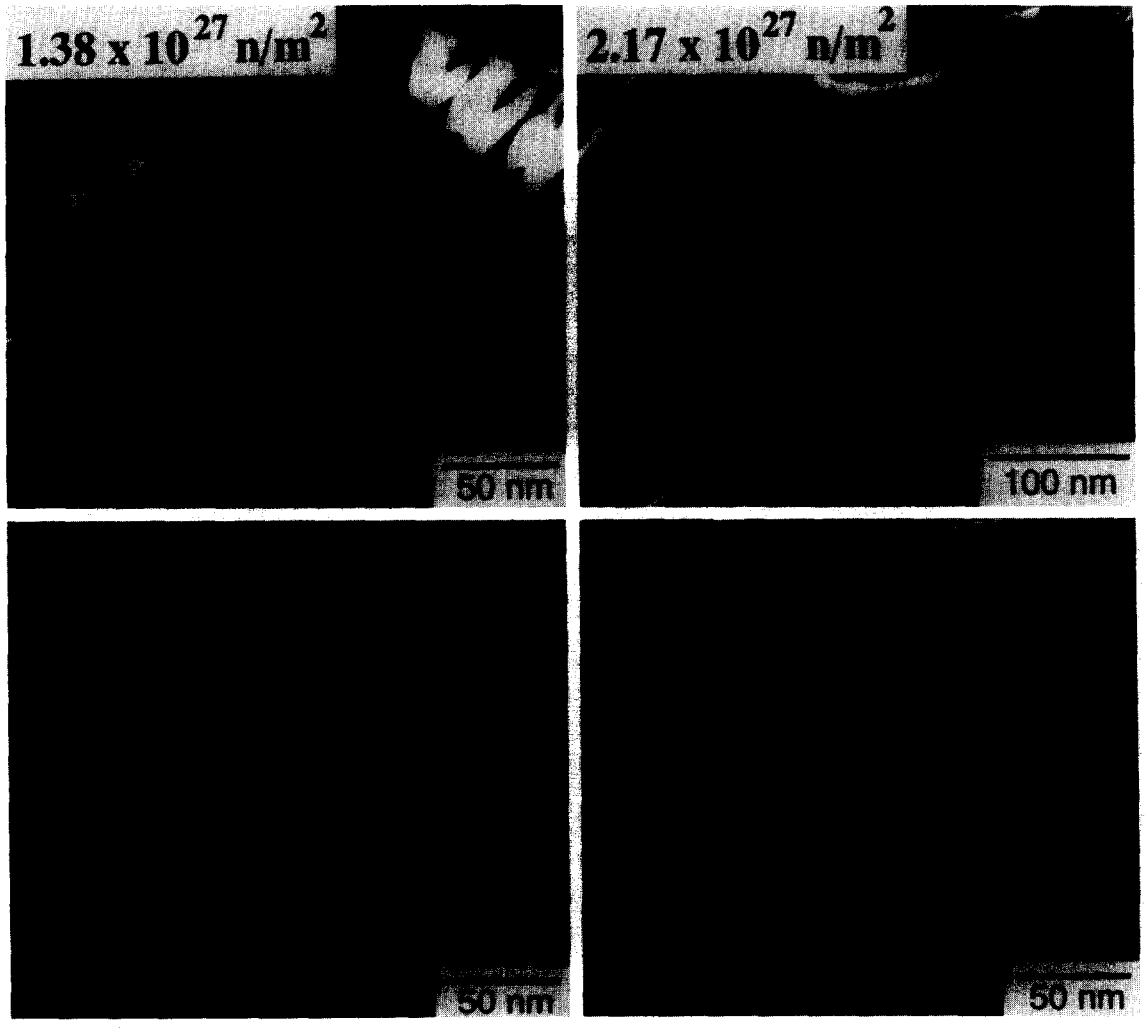

Fig. 10. Weak-beam dark-field (upper) and kinematical bright-field (lower) micrographs showing stacking fault networks (upper) and voids (lower) in $MgAl_2O_4$ irradiated in FFTF at 1023 K to 1.38×10^{27} n/m^2 (left) and 2.17×10^{27} n/m^2 (right), respectively.

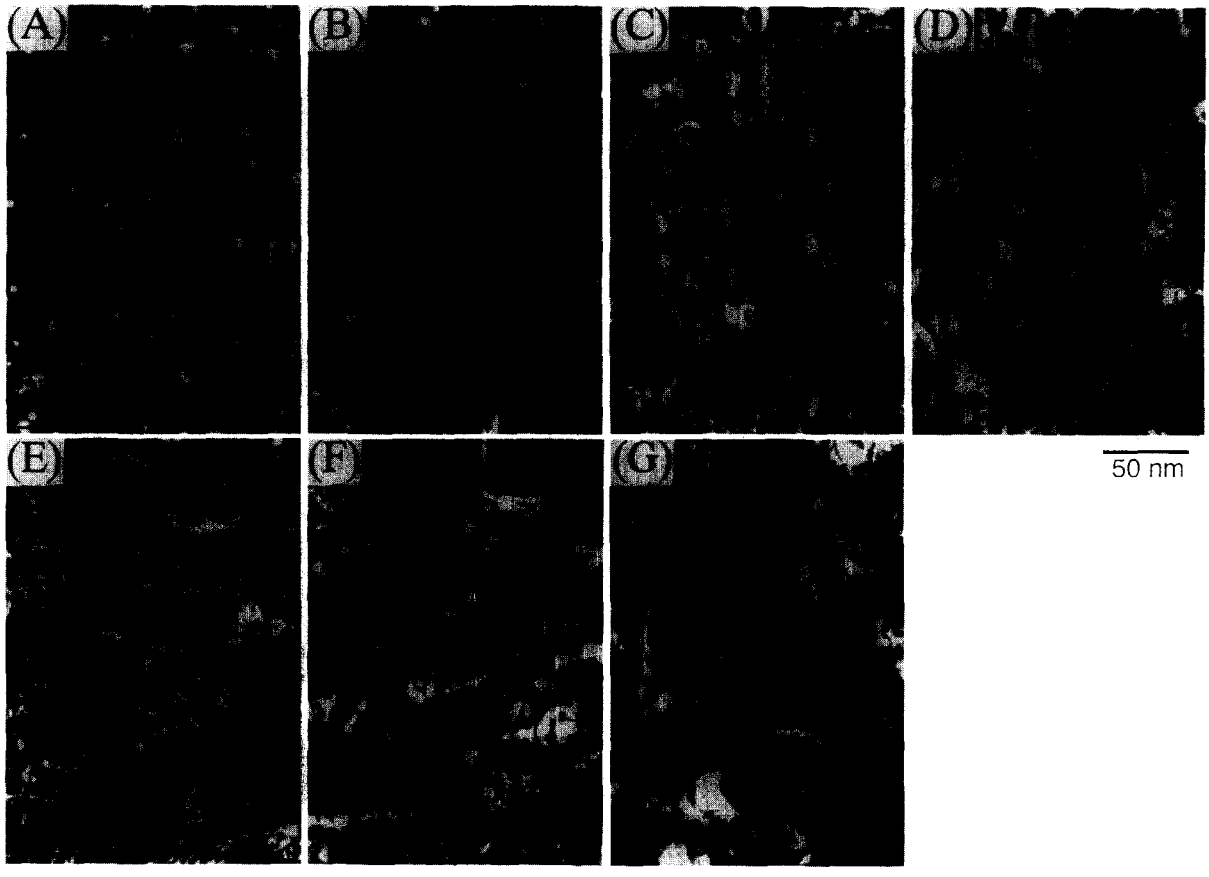

Fig. 11. Typical examples of weak-beam dark-field micrographs showing interstitial dislocation loops in α-Al_2O_3 irradiated in JOYO to (a) 7.6×10^{23} n/m^2 at 673 K, (b) 7.5×10^{24} n/m^2 at 673 K, (c) 7.5×10^{24} n/m^2 at 773 K, (d) 7.5×10^{24} n/m^2 at 873 K, (e) 5.49×10^{25} n/m^2 at 673 K, (f) 5.49×10^{25} n/m^2 at 773 K and (g) 5.49×10^{25} n/m^2 at 873 K.

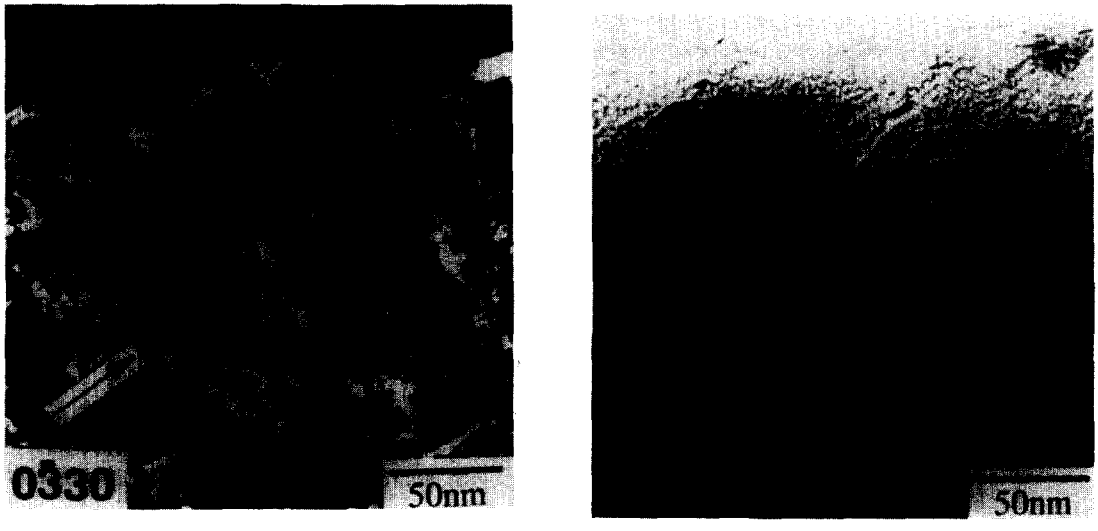

Fig. 12. Weak-beam dark-field (left) and kinematical bright-field (right) micrographs showing dislocation networks and voids in α-Al_2O_3 irradiated in JOYO to 5.49×10^{25} n/m^2 at 673 K, respectively.

tional change around stacking faults. The $\frac{1}{4}[110](111)$ loops are mixed dislocation loops which have Burgers vector with both edge and screw components. In order to reduce the dislocation energy and the stacking fault energy, $\frac{1}{4}[110](111)$ mixed loops rotate their habit planes through glide cylindrical motion and convert into $\frac{1}{4}[110](110)$ prismatic loops. It is considered that $\frac{1}{4}[110](101)$ mixed loops are formed on the way to rotating the plane from the (111) to (110) planes along the glide cylinder, and that $\frac{1}{4}[110](101)$ loops are metastable and are consequently converted into $\frac{1}{4}[110](110)$ prismatic loops. The $\frac{1}{4}[110](110)$ loops maintain the stoichiometry of $MgAl_2O_4$ and the electrical neutrality, so that $\frac{1}{4}[110](110)$ loops are stable and able to grow into large loops a few hundred nm in diameter.

Fig. 14 summarizes the character of defect clusters in $MgAl_2O_4$ and α-Al_2O_3 as functions of irradiation temperature and neutron fluence, including data published by others [1,2]. The curved lines in the figure denote the threshold for observable void formation in $MgAl_2O_4$ and α-Al_2O_3. A high density of interstitial loops, including unfaulted perfect loops, are formed in α-Al_2O_3 irradiated to relatively low neutron fluences. The early nucleation of interstitial loops induces excess vacancies to nucleate voids. The bias factor promoting such segregation is proportional to the magnitude of the Burgers vector of dislocation loops [21]. So, the perfect $\frac{1}{3}\langle 10\bar{1}1\rangle$ loops formed in α-Al_2O_3 act as more efficient interstitial sinks than do unfaulted loops. The threshold fluence for void formation in α-Al_2O_3 therefore corresponds to the fluence required for formation of perfect loops. In $MgAl_2O_4$ irradiated to much higher exposures in FFTF, however, a low density of faulted loops remain to high neutron fluences, and the appearance of perfect loops is not always correlated with the formation of voids. The threshold fluence for void formation in $MgAl_2O_4$ is about two orders of magnitude higher than α-Al_2O_3.

It appears that the formation of stable interstitial loops in $MgAl_2O_4$ occurs only seldomly under neutron irradiation conditions, mainly because of the more effective direct recombination of interstitials and structural vacancies. This reduced formation rate is also due to the large critical nucleus of stable interstitial loops. Decreased formation of stable interstitial loops enhances the recombination of interstitials and vacancies and thereby suppresses the formation of vacancy clusters. The insignificant role of uniform ionizing radiation on the nucleation and growth process of defect clusters in $MgAl_2O_4$ has been described elsewhere [22].

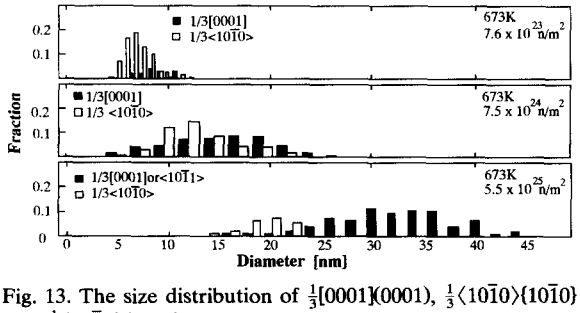

Fig. 13. The size distribution of $\frac{1}{3}[0001](0001)$, $\frac{1}{3}\langle 10\bar{1}0\rangle\{10\bar{1}0\}$ and $\frac{1}{3}\langle 10\bar{1}1\rangle(0001)$ types of interstitial dislocation loops in α-Al_2O_3 irradiated in JOYO to 7.6×10^{23}, 7.5×10^{24} and 5.49×10^{25} n/m^2 at 673 K.

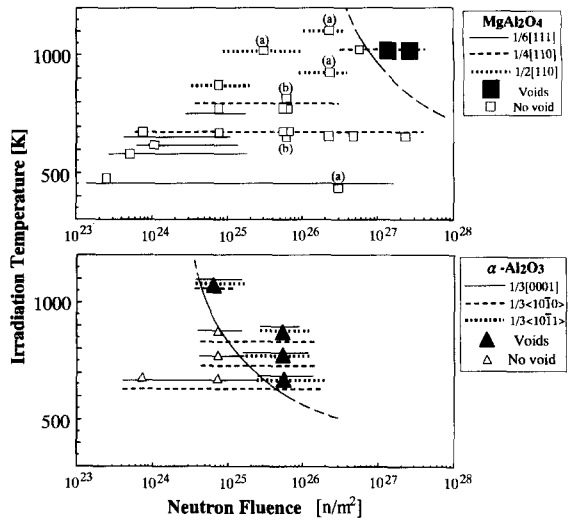

Fig. 14. A summary of the character of dislocation loops and the critical fluence of the formation of voids for $MgAl_2O_4$ and α-Al_2O_3 as functions of irradiation temperature and neutron fluence. (a) and (b) are based on the result by Clinard, Jr. et al. [1] and Parker et al. [2], respectively. The result on α-Al_2O_3 by Youngman et al. [17] is not shown in the figure, but is consistent with the present result.

5. Conclusions

The strong resistance to void swelling of $MgAl_2O_4$ under irradiation has been confirmed to approximately 230 dpa, and the causative mechanism has been investigated by comparing the nucleation and growth process of defect clusters in low swelling $MgAl_2O_4$ and high swelling α-Al_2O_3. The following conclusions have been drawn.

(1) The $\frac{1}{6}\langle 111\rangle$ type of interstitial loops nucleate in $MgAl_2O_4$ but then follow the following growth process to reduce the energy of individual loops;

$$\tfrac{1}{6}[111](111) \rightarrow \tfrac{1}{4}[110](111) \rightarrow \tfrac{1}{4}[110](101) \rightarrow \tfrac{1}{4}[110](110) \rightarrow \tfrac{1}{2}[110](110).$$

(2) The fraction of displacements retained in the form of interstitial dislocation loops in $MgAl_2O_4$ at relatively high exposure levels is extremely small, being less than 0.02% under those experimental conditions.
(3) No voids are formed in $MgAl_2O_4$ irradiated at 1023 K to 5.6×10^{26} n/m^2, but very small voids precipitate not only along the $\frac{1}{4}\langle 110\rangle\{110\}$ stacking faults but also in the matrix when irradiated at 1023 K to 1.38×10^{27} n/m^2.
(4) The diameter and the density of voids in $MgAl_2O_4$ irradiated at 1023 K to 2.17×10^{27} n/m^2 ($\sim$ 220 dpa) are estimated to be 6–8 nm and 4×10^{24} voids/m^3, respectively, comprising a void swelling volume of only 0.07%.
(5) In α-Al_2O_3, faulted $\frac{1}{3}\langle 10\bar{1}0\rangle\{10\bar{1}0\}$ and $\frac{1}{3}[0001](0001)$ interstitial loops nucleate and grow into perfect $\frac{1}{3}\langle 10\bar{1}1\rangle(0001)$ loops.
(6) The nucleation of a high density of voids in α-Al_2O_3 occurs for neutron fluences less than 7.5×10^{24} n/m^2 at 873 K and is correlated with the appearance of perfect loops.
(7) The large difference in dislocation loop evolution appears to account for the ease of void swelling in α-Al_2O_3 and the strong resistance to void formation in $MgAl_2O_4$.
(8) Constraints unique to the $MgAl_2O_4$ crystal structure do not allow the formation of dislocation network structures that favor swelling.

Acknowledgements

This research was supported by a Grant-in-Aid for Fusion Research by the Ministry of Education, Science and Culture of Japan. One of the authors (KF) was also supported by the JSPS Fellowships for Japanese Junior Scientists. The authors are deeply indebted to the staff members of the Oarai Facility of the IMR, Tohoku University, especially to Messrs. M. Narui and T. Shibayama for their experimental assistance. The irradiation in FFTF and the participation of F.A. Garner were supported by the office of Fusion Energy, US Department of Energy under contract DE-AC06-76RLO-1830.

References

[1] F.W. Clinard, Jr., G.F. Hurley and L.W. Hobbs, J. Nucl. Mater. 108&109 (1982) 655.
[2] C.A. Parker, L.W. Hobbs, K.C. Russell and F.W. Clinard, Jr., J. Nucl. Mater. 133&134 (1985) 741.
[3] L.W. Hobbs and F.W. Clinard, Jr., J. Phys. 41 C 6 (1980) 232.
[4] S.J. Zinkle, Nucl. Instr. and Meth. B 91 (1994) 234.
[5] F.A. Garner, G.W. Hollenberg, J.L. Ryan, Z. Li, C.A. Black and R.C. Bradt, J. Nucl. Mater. 212–215 (1994) 1087.
[6] F.A. Garner, G.H. Hollenberg, K. Black and R.C. Bradt, in these Proceedings, J. Nucl. Mater.
[7] M. Kiritani, J. Nucl. Mater. 160 (1988) 135; also M. Kiritani, Y. Yoshiie, S. Kojima, Y. Satoh and K. Hamada, J. Nucl. Mater. 174 (1990) 327.
[8] F.A. Garner, N. Sekimura, M.L. Grossbeck, A.M. Ermi, J.W. Newkirk, H. Watanabe and M. Kiritani, J. Nucl. Mater. 205 (1993) 206.
[9] K. Fukumoto, Doctor Thesis, Kyushu University (1994).
[10] T.E. Mitchell, J. Am. Ceram. Soc. 62 (1979) 254.
[11] D.M. Maher and B.L. Eyre, Philos. Mag. 23 (1971) 409.
[12] L.W. Hobbs, A.E. Hughes and D. Pooley, Proc. R. Soc. London A 332 (1973) 167.
[13] K. Fukumoto, Doctor Thesis, Kyushu University (1994).
[14] R.S. Wilks, J.A. Desport and R. Bradley, Proc. Brit. Ceram. Soc. 7 (1967) 403.
[15] R.S. Wilks, J. Nucl. Mater. 26 (1968) 137.
[16] D.J. Barbat and N.J. Tighe, J. Am. Ceram. Soc. 51 (1968) 611.
[17] R.A. Youngman, T.E. Mitchell, F.W. Clinard, Jr. and G.F. Hurley, J. Mater. Res. 6 (1991) 2178.
[18] C. Kinoshita and K. Nakai, Jpn. J. Appl. Phys. series 2 (1985) 105.
[19] P. Veyssiere, J. Rabier and J. Grilhe, Phys. Status Solidi A 31 (1975) 605.
[20] P. Veyssiere, J. Rabier, H. Garem and J. Grilhe, Philos. Mag. 38 (1978) 61.
[21] A.H. Cottrel and B.A. Bilby, Proc. Phys. Soc. 62 (1949) 49.
[22] C. Kinoshita, H. Abe, S. Maeda and K. Fukumoto, in these Proceedings, J. Nucl. Mater. 219 (1995) 152.